



Numerical performance evaluation of tubular solar still with different geometries of water basin

Shaik Subhani, Rajendran Senthil Kumar*

Department of Mechanical Engineering, SRM IST, Chennai, India, Tel. +91 9962280030/+91 9952156288;
emails: senthilr2@srmist.edu.in (R. Senthil Kumar), subhanishaik9900@gmail.com (S. Subhani)

Received 3 December 2019; Accepted 8 April 2020

ABSTRACT

There is a rapid increase in population on earth, which leads to the rapid consumption of fresh-water resources that are naturally available to be 3% of the total water on our planet. Also, there is a problem with the pollution of water resources due to sewers leakage, pesticide runoffs, etc. Conventional stills have limitations due to low productivity. Hence research and development are being conducted to enhance the productivity of stills. The works of literature reported that numerical and flow analysis of heat transfer in tubular still and concluded that productivity is sensitive to the glass surface, basin water temperature and also the sharp corners in the sloped solar stills. So, a new modified curved surface under the basin has been implemented which helps in supporting the basin and also in condensing the evaporated water inside the still. The present research addresses the heat and fluid flow inside a still due to geometrical modifications are done on the basin and compares the performance of each design by varying the location of it ($D/2$ and $D/3$) as shown. The solar still performs best when the curved water basin is at $1/2$ nd of the still diameter at higher Rayleigh numbers. When compared to conventional stills, the tubular still with a linear basin at $D/2$ dissipates 31.4% more heat. This means a better production rate of solar stills at higher Rayleigh numbers.

Keywords: Solar still; Tubular design; CFD; Heat transfer; Fluid flow

1. Introduction

Nowadays water depletion is the most common problem faced by the major areas in the world and most of the available water is not ready to be consumed directly or safe enough. Also, available water needs to be treated first before using it, so there are many ideas to develop potable water from saline water. Desalination is a technique in which energy is used to remove the impurities and thus producing potable water. As solar energy is mostly available as energy resources in remote areas, the desalination process using solar energy is very useful and also cost-effective than other desalination techniques. Many researchers have been working on improving the productivity of the solar

still and developed different types of stills for a better production rate. This study relates to tubular solar still and its performance analysis where solar stills are modified for performance improvement. Sanjeev and Tiwari [1] have done a theoretical analysis and further developed a model and optimized depth of water and exposed area using computer simulations. Ismail [2] experimentally analyzed the hemispherical solar still and concluded their results with an 8% depletion of production rate and a 50% increase in depth in solar still. Esfahani and Bordbar [3] studied transportable solar stills induced with heat pipe and thermoelectric module at the condensing surface. Abdenacer and Nafila [4] analyzed and concluded that the maximum production rate can be achieved at the maximum temperature difference

* Corresponding author.

Presented at the First International Conference on Recent Trends in Clean Technologies for Sustainable Environment (CTSE-2019), 26–27 September 2019, Chennai, India

between evaporating and condensing surfaces. Al-Garni et al. [5] studied solar stills and reported that there is an inverse effect on productivity concerning water depth and also claimed that the angle of glass can also be optimized. Dwivedi and Tiwari [6] experimentally studied by comparing heat transfer coefficients internally in passive solar stills at three water depths and reported that there are fewer differences in heat dissipation coefficients at increasing water depths. Bhardwaj et al. [7] experimentally investigated the effects of changing the condensation area on solar still for water production and concluded the unavoidable effect on the production rate with the increase in the condensing surface. Heydari and Rahbar [8] studied the effect on vertical walls with water injection including time intervals on single slope solar still and concluded performance can be enhanced by 7%. Papanicolaou and Belessiotis [9,10] numerically simulated solar still with a single slope and studied the flow structure of the double-diffusive natural convection unit. Rashidi et al. [11,12] studied and optimized the configuration of the solar still using both computational fluid dynamics and response surface methods. Fotouhi-Bafghi and Rahbar [13] and Rahbar et al. [14] have done the numerical study on the performance by simulating different geometries of tubular solar stills and projected best of them after studying convective heat and mass transfer coefficients. Ahsan and Fukuhara [15] and Ahsan et al. [16] suggested a new design using the humid air concept to evaluate different parameters like vapor density, relative humidity and temperature variations of tubular solar still for better production rate. Subhani and Senthil Kumar [17] numerically analyzed the single slope solar still performance after adding baffles at different locations with constant temperature difference and variable temperature difference and concluded that the performance of still is appreciable when the baffle is at half of the basin length with minimum fluctuations in production rate. Rahbar et al. [18] compared and studied the results of solar stills of two different types (tubular and triangular) after testing experimentally considering ambient temperature and solar radiation effects on the productivity of water and efficiency. They concluded that tubular solar still has a 20% more production rate than the triangular one. As the angle of the solar still has also influenced the heat transfer rate significantly, due to the variation of characteristic length responsible for heat transfer. Considering this statement, our study concentrates on the evaluation of tubular solar still, as they are providing lots of interest in researchers and easy to construct.

While they have a better angle to ease the condensate to be collected. Although the performance has been optimized by altering the geometries and condensation techniques, there is more scope in optimizing basin height and adding partition inside the tubular solar still using the analysis of flow structure and heat transfer correspondingly. Hence, two different configurations of the water basin in tubular solar still were considered and analyzed in this study.

2. Problem statement

In this study, a solar still with single slope condensing surface (Fig. 1) has been considered first for analysis and compared the results with modified design parameters for tubular solar still with different water basin heights as shown in Fig. 2. The numerical study was carried out using Ansys Fluent – 18. Here, the flow is 2-dimensional, laminar, and steady. Thermo-physical properties of the fluid are taken at a mean temperature between evaporating and condensing surfaces. The schematic representation of solar stills with non-dimensionalized design parameters considered in this study is shown below. Single slope solar still with design parameters of left side height L_H , right side height R_H and separation between the walls are L_L as shown in Table 2 and temperatures at the top and bottom walls are T_T and T_B respectively, where side walls are considered to be adiabatic as shown in Fig. 1. Now, by maintaining the same area as single slope solar still (Fig. 1) considered before, the sloped condensing surface has been modified into the tubular surface as shown in Fig. 2 with a tube diameter of D with both linear and curved basin structures and a water depth of around 2cm. The further study has been done by relocating the still's linear and curved basins from the $D/2$ location to the $D/3$ location. Linear water basin with a total length of L ($=D-4.1$ cm) and with basin height of H ($=10\%$ of L) is studied first and followed by a curved water basin by maintaining the same flow revolving area as the previous one as shown. Due to symmetricity, the half portion of the 2D design is simulated and also to create a chambered gap inside the tubular solar still, a partition is provided for the entire diameter of the still.

3. Governing equations and solving procedure

The common governing equations for heat transfer and fluid flow is condensed to two-dimensional form after assuming suitable assumptions as represented in Eqs. (1)–(4)

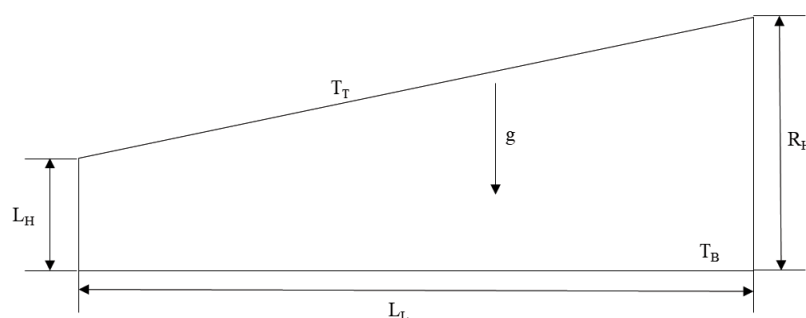


Fig. 1. Conventional solar still (single slope).

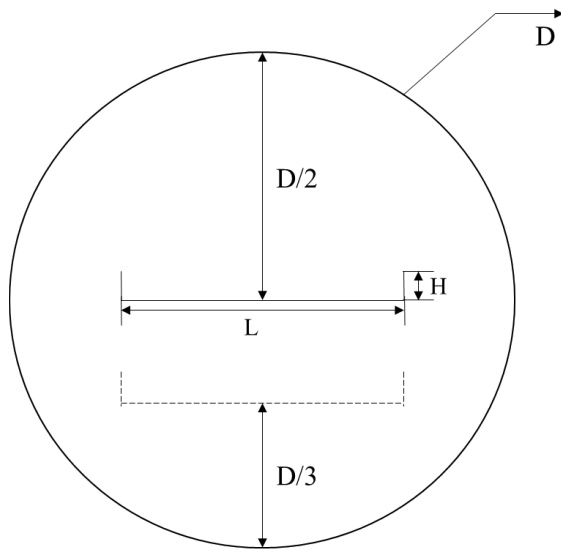


Fig. 2. Tubular solar still with linear basin.

Continuity equation:

$$\frac{\partial u}{\partial x} + \frac{\partial v}{\partial y} = 0 \quad (1)$$

X-momentum equation:

$$\rho \left(u \frac{\partial u}{\partial t} + v \frac{\partial u}{\partial y} \right) = -\frac{\partial p}{\partial x} + \mu \left(\frac{\partial^2 u}{\partial x^2} + \frac{\partial^2 u}{\partial y^2} \right) \quad (2)$$

Y-momentum equation:

$$\rho \left(u \frac{\partial v}{\partial t} + v \frac{\partial v}{\partial y} \right) = -\frac{\partial p}{\partial y} + \mu \left(\frac{\partial^2 v}{\partial x^2} + \frac{\partial^2 v}{\partial y^2} \right) + g\beta(T - T_\infty) \quad (3)$$

Energy equation:

$$u \left(\frac{\partial T}{\partial x} \right) + v \left(\frac{\partial T}{\partial y} \right) = \alpha \left(\frac{\partial^2 T}{\partial x^2} + \frac{\partial^2 T}{\partial y^2} \right) \quad (4)$$

The discretization of equations and solving is done using the finite volume method with suitable assumptions. Here walls are imposed with no-slip boundary conditions and also vertical walls are considered as adiabatic to resemble the insulation. The second-order upwind scheme is used for discretization of the governing equations whereas the SIMPLE algorithm is used for coupling pressure and velocity. The residuals for the mass (10^{-6}), momentum (10^{-6}) and energy (10^{-12}) respectively are preferred to reduce the error level.

Formulae:

$$Nu = \frac{hL}{k} \quad (5)$$

$$Ra = \frac{g \cdot \beta \cdot (T - T_\infty) \cdot L^3}{\nu \cdot \alpha} \quad (6)$$

4. Grid generation and grid independence

As the considered problem consists of sharp protrusions at the basin and curved condensing surface, the triangular unstructured elements meshed using Ansys Workbench are preferred. To analyze the precise heat transfer and flow physics, the more refined mesh has been preferred nearer to the walls (Fig. 3). Also, a complete grid convergence study is carried (Table 1) by altering the number of elements to reduce the error percentage. Among which the total elements (37908) show the fewer variations in output and hence considered as the limit for the grid convergence (within the limit).

5. Result and discussion

5.1. Validation of the study

Rashidi et al. [11] and Rahbar and Esfahani [19] reported the plain solar still performance with measurements of 18.7 and 7.5 cm on the right side and left side respectively and parting of 43.8 cm between them. The present measurement therefore related and checked solar still performance in Table 2. Now, the present findings of the computation suit literature closely.

5.2. Analysis of solar still performance (at constant temperature difference)

The current study was proceeded by relating temperature and velocity contours of a solar still with a single slope by varying condensing and evaporating surfaces at a constant difference in temperature. First, for analysis, a conventional still was considered. Here, a bi-cellular non-uniform flow structure, with axis normal to the condensing surface (Fig. 4) is found when 10°C temperature

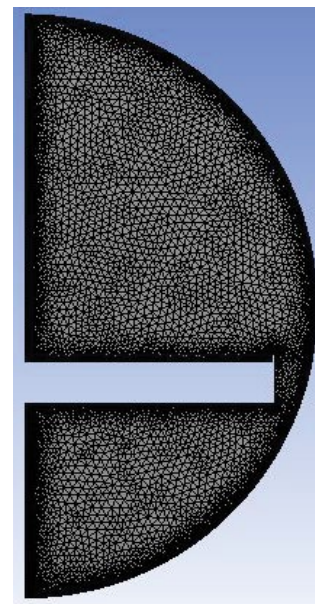


Fig. 3. Mesh distribution in tubular solar still with a linear basin at $D/3$.

Table 1
Study of grid independence

Mesh elements	Nu	% of variation
29,197	11.4362	–
35,117	11.376	0.526
37,908	11.415	0.342
42,644	11.4	0.131
47,672	11.39	0.09

Table 2
Present computation validation with literature

T_T (°C)	48
L_L (m)	0.438
T_B (°C)	63
Nu (Rashidi et al. [11])	10.5
Nu (Rahbar and Esfahani [19])	10.7
Nu (present study)	10.4
Percentage of variation	2.8% and 0.95%

difference is maintained ($T_T = 30^\circ\text{C}$ and $T_B = 40^\circ\text{C}$). On progressively increasing the temperature of condensing and evaporating surfaces to 40°C and 50°C respectively, the major variations do not significantly affect fluid flow structure along with velocity, vorticity (Fig. 4) and convective performance (Table 3). Presently, the conventional solar still is redesigned into tubular by maintaining the same area and further analysis has been done for different basin structures. Exactly when the linear basin is in the middle of the still diameter, the water and glass surfaces at 40°C and 30°C and the gap between the evaporating and condensing surface is minimized, bi-cellular non-uniform

vortices (Fig. 5) have been observed. The heat transfer rate (Table 3) has also been increased at lower temperatures itself with lesser vorticity and velocity magnitudes (Fig. 6) as compared to single slope solar still. When temperature agitation is further increased from 60°C and 70°C for water surface and 50°C and 60°C for glass surface, the same type of flow pattern (Fig. 5) can be observed but because of the higher agitation, the fluid in bottom portion also gets involved in the heat transfer. Thus, resulting in the depletion of heat transfer rate (Table 3) towards glass cover from the water surface gradually.

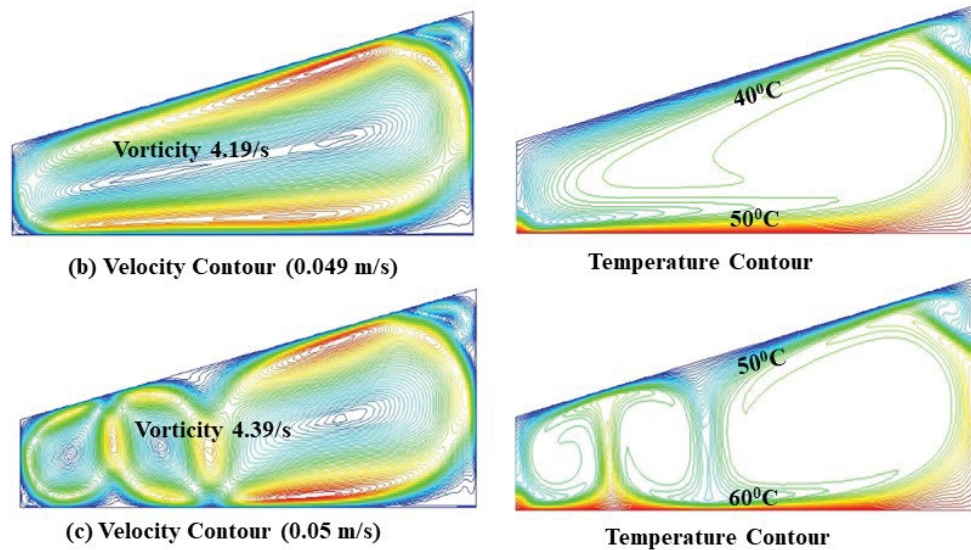


Fig. 4. Contours in conventional still (velocity and temperature).

Table 3
Nu vs. Ra at constant temperature difference for conventional and tubular stills

Bottom wall temperature (°C)	Rayleigh number (10^3)	Nusselt number				
		Conventional still	Linear water basin		Curved water basin	
			Basin at $D/2$	Basin at $D/3$	Basin at $D/2$	Basin at $D/3$
40	2,722.345	9.368	12.67	11.809	13.26	12.823
50	2,350.932	9.38	12.218	11.71	12.805	12.249
60	2,040.387	12.17	11.799	11.625	12.379	11.748
70	1,779.32	12.22	11.415	11.051	13.363	11.32

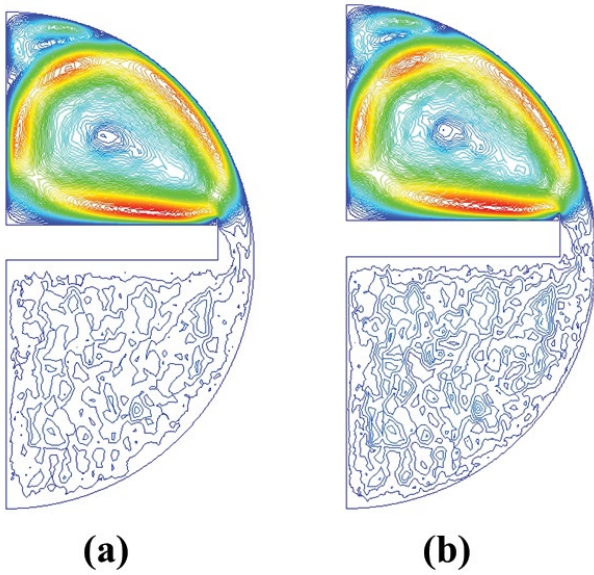


Fig. 5. Velocity contours for tubular solar still with a linear basin at D/2. (a) WT = 40°C; GT = 30°C and (b) WT = 50°C; GT = 40°C.

When the linear water basin is at 1/3 of the still diameter and water surface and glass cover temperatures are 40°C and 30°C respectively, the same bi-cellular non-uniform flow structure (Figs. 7 and 8) has been seen but with larger magnitude (Fig. 6) and radii, where the smaller vortex is not effectively participating in carrying energy from hot wall to cold wall. Thus reducing heat transfer rate (Table 3). But as long as the vorticity magnitude increases, the fluctuations created by the solar radiation can be tackled by decreasing the variations at the end production rate. Also by increasing the velocity and vorticity magnitudes (Fig. 6), the heat transfer rate further decreases with

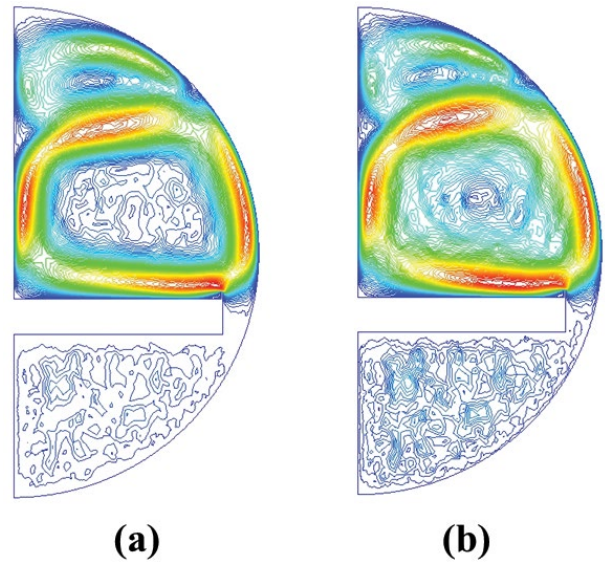


Fig. 7. Velocity contours for tubular solar still with a linear basin at D/3. (a) WT = 40°C; GT = 30°C and (b) WT = 60°C; GT = 50°C.

increasing temperatures at both water surface and glass cover surface with the same flow pattern (Figs. 7 and 8) inside the still. Analysis has been continued by modifying the linear water basin into a curved water basin by maintaining the same area as before. When the curved water basin is at 1/2nd of the still diameter, exactly at water surface temperature of 40°C and glass cover temperature of 30°C, the same non-uniform bi-cellular vortices (Fig. 9) observed in linear water basin with increased heat transfer rate (Table 3) by maintaining almost the same magnitudes of velocity and vorticity (Fig. 6). For further increase in surface temperatures at glass cover and water surface at a constant

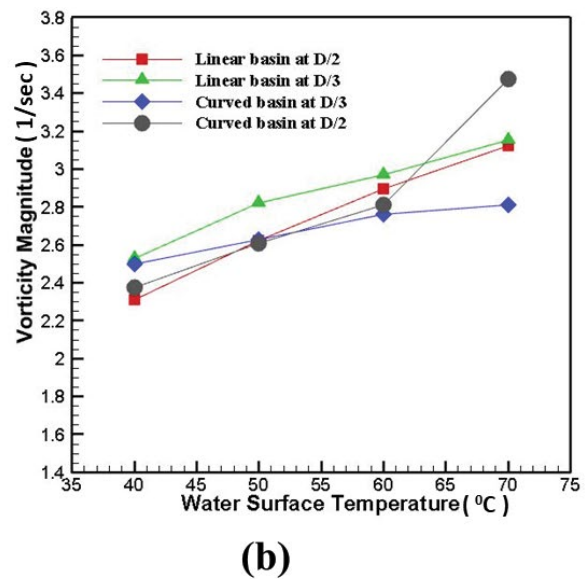
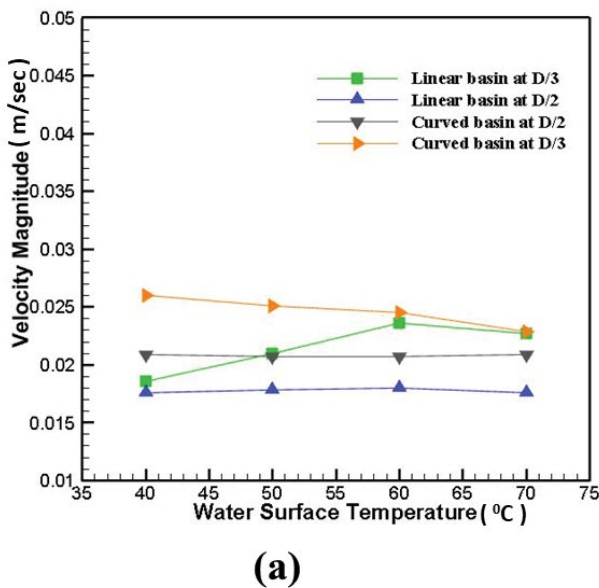


Fig. 6. Respective magnitudes of tubular solar still with different basins at constant temperature difference. (a) Velocity magnitude (m/s) reference to water surface temperature (°C) and (b) vorticity magnitude (1/s) reference to water surface temperature (°C).

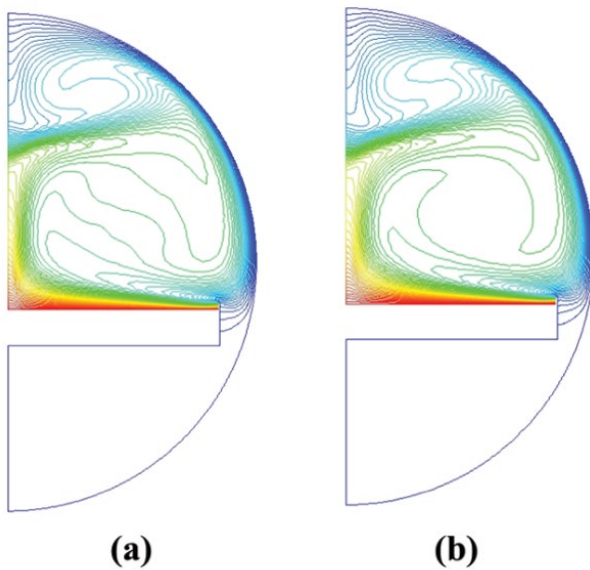


Fig. 8. Temperature contours for tubular solar still with a linear basin at $D/3$. (a) WT = 40°C; GT = 30°C and (b) WT = 70°C; GT = 60°C.

difference of 10°C (40°C–50°C and 50°C–60°C respectively), the pattern observed is retained. However, due to fluid interaction and agitation at the bottom of the basin (Fig. 9), the rate of heat transfer can be seen to decline (Table 3).

Furthermore, with an increase in wall temperature to a maximum of 70°C at the water surface and 60°C at glass cover, the flow structure gets more concentrated towards the walls of the still by appreciable improvement in the velocity and vorticity magnitudes (Fig. 6). Thus, the fluid effectively participates in the energy-carrying process and thereby increases the heat transfer rate. When the curved water basin is at $1/3$ of the still diameter, exactly at water surface temperature of 40°C and glass cover temperature 30°C, bi-cellular non-uniform vortices with larger radii (Figs. 10 and 11) and a dull zone nearer to the glass surface results in performance deterioration in rate of heat transfer (Table 3) although the velocity and vorticity magnitude are increased and compared with a basin at $1/2$ of the still diameter.

Furtherly, for constant increase in the water surface and glass cover temperature, there is no change in the flow pattern and also due to increase in agitation the fluid below the basin has also started participating in the heat transfer process, thereby resulting in a constant reduction of transfer of heat between the glass cover and water surface but with a gradual increase in velocity and vorticity magnitudes (Fig. 6) at respective temperature differences.

5.3. Analysis of solar still performance (at variable temperature difference)

The still performance was studied after varying the temperature differences of the condensing and evaporating wall temperatures from 25°C–90°C. Now, in plain still, more vortices responsible for heat transfer enhancement are produced at a lower fluid velocity, lower wall temperatures.

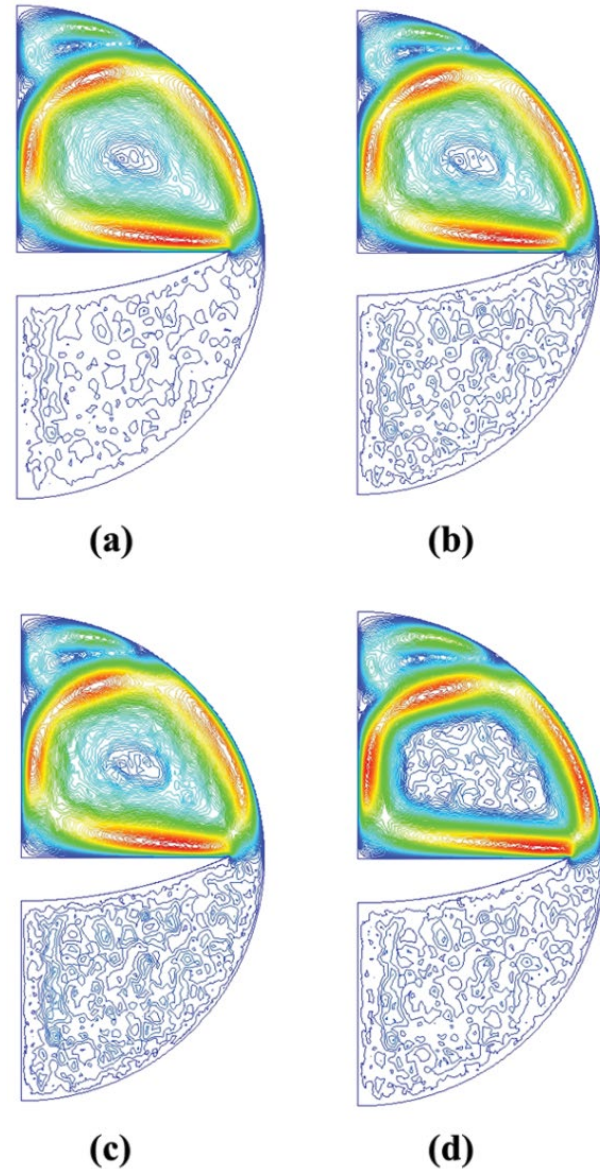


Fig. 9. Velocity contours for tubular solar still with a curved basin at $D/2$. (a) WT = 40°C; GT = 30°C, (b) WT = 50°C; GT = 40°C, (c) WT = 60°C; GT = 50°C, and (d) WT = 70°C; GT = 60°C.

In contrast, the rise in variation in temperature contributes to the vortices merging (Fig. 12) in response to a reduction in the transfer of heat by almost 19% (Fig. 13). A further rise in agitation due to temperature provides desirable vorticity (Fig. 12) with an increment in magnitudes, with significant enhancement in the transfer of heat, velocity, and degree of vorticity. The vortices converge and form a bi-cellular flow system at higher temperatures, the direction of which is normal to the condensing layer, where the natural convection inside is not significantly increased. When the linear water basin is at $1/2$ of the still diameter, exactly at lower temperature differences (25°C and 30°C at glass cover and 30°C and 40°C at water surface temperature) two non-uniform revolving vortices concentrated nearer to the walls (Fig. 14) have been observed. Furthermore, on increasing

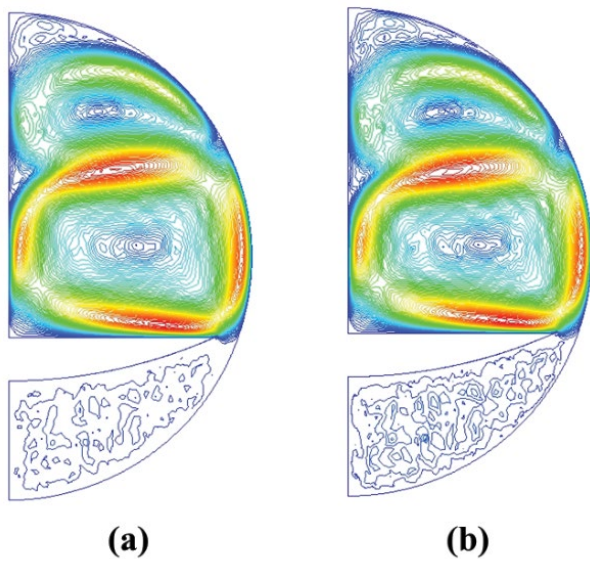


Fig. 10. Velocity contours for tubular solar still with a curved basin at $D/3$. (a) $WT = 40^\circ\text{C}$; $GT = 30^\circ\text{C}$ and (b) $WT = 50^\circ\text{C}$; $GT = 40^\circ\text{C}$.

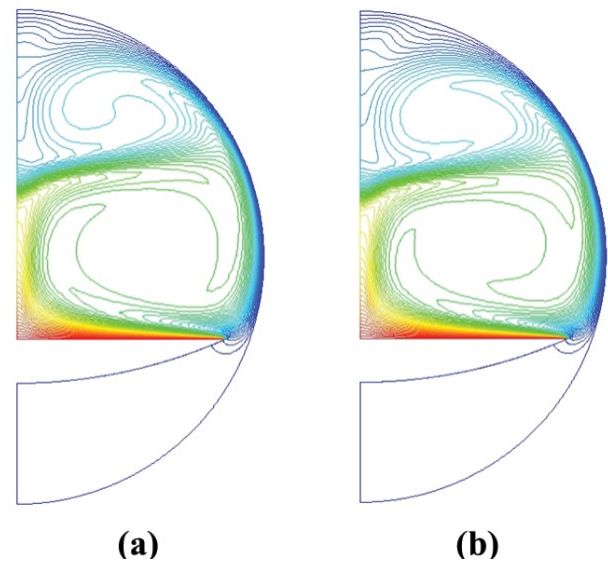


Fig. 11. Temperatures contours for tubular solar still with curved basin at $D/3$. (a) $WT = 40^\circ\text{C}$; $GT = 30^\circ\text{C}$ and (b) $WT = 50^\circ\text{C}$; $GT = 40^\circ\text{C}$.

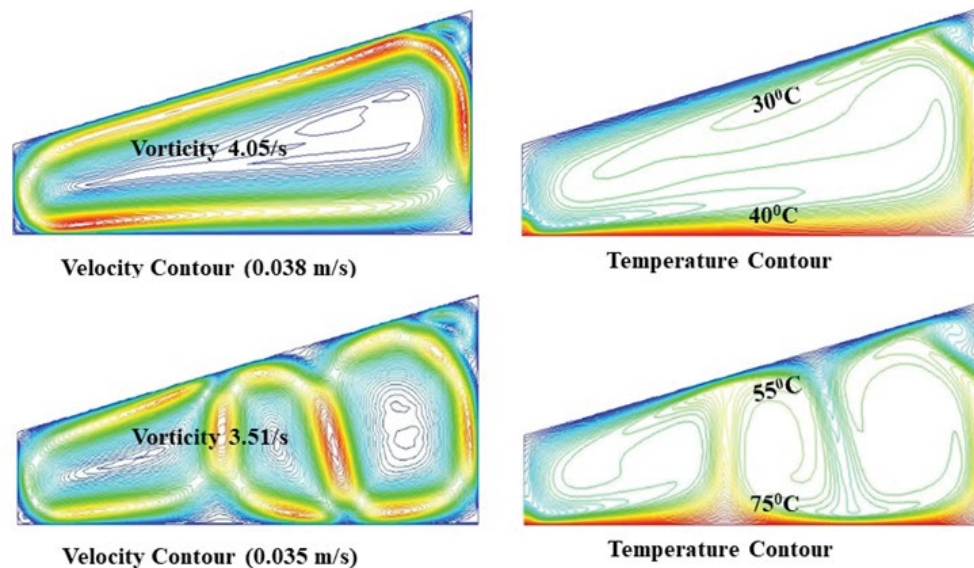


Fig. 12. Contours in conventional still (velocity and temperature).

the temperature differences, the same type of flow pattern with a gradual increase in velocity and vorticity magnitude (Fig. 15) has been observed. Enhancement of heat transfer rate is also observed as the appreciable fluid interaction between the water surface and glass surface (Fig. 14) is more. With the increase in temperature difference, the fluid below the water basin is also participating effectively, thus resulting in minimum significant improvement of natural convection.

When the linear water basin is at $1/3$ of the still diameter at lower temperature differences, there is an effective enhancement of convection rate than the single slope solar still but not much as still with a basin at $1/2$ of diameter.

However, the rate of fluctuations created in the previous case has been reduced as there is more space for the fluid to establish a complete flow pattern between the water surface and glass surface (Figs. 16 and 17) with a constant increase in velocity and vorticity magnitude (Fig. 15).

Again at higher temperature differences, even though the vorticity and velocity magnitudes are increasing gradually (Fig. 15) and even better than basin at $1/2$, the heat transfer enhancement is not much appreciable than the previous one because there is an increase in the area of the dull zone and non-interacting vortices nearer to the glass surface (Figs. 16 and 17).

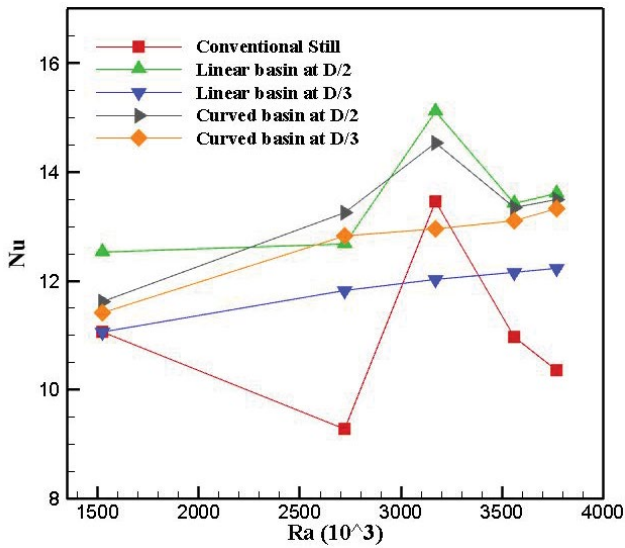


Fig. 13. Nu vs. Ra plot for variable temperature differences.

When the curved water surface is at the middle, at lower temperature differences, the still's performance is not effectively enhanced when compared with the linear water basin but has an improvement when compared with conventional single slope solar still at lower velocity magnitudes. On increasing the temperature differences in the still, there is no effective change in the flow pattern (Fig. 18), when compared with a linear water basin and shows similar velocity and vorticity magnitudes (Fig. 13) with the same fluid flow interactions. Whereas, when the curved water basin is positioned at 1/3 of diameter, at lower temperature differences, due to low agitation the fluid interaction between the hot wall and cold wall (Fig. 19) is not effective in heat transfer enhancement due to increase in the area provided from heat transfer. At higher temperature differences,

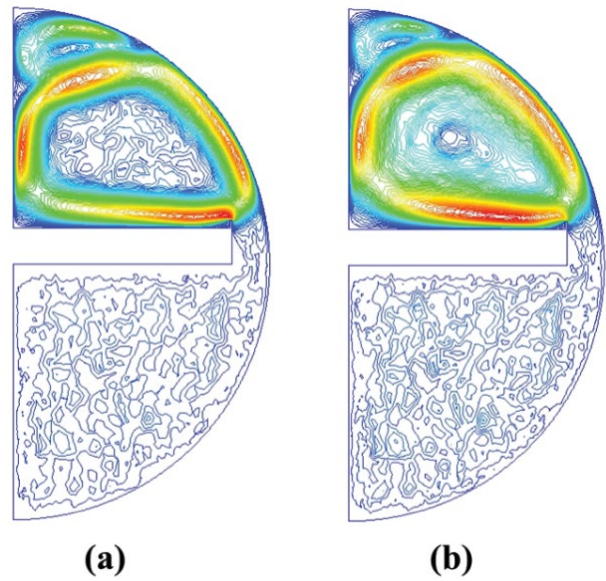


Fig. 14. Velocity contours for tubular solar still with a linear basin at D/2. (a) WT = 45°C; GT = 60°C and (b) WT = 55°C; GT = 75°C.

the vortices formed influence heat transfer enhancement but not as much when compared to the curved basin at 1/2. The final heat transfer rate is enhanced (Fig. 13) on increasing the temperature differences and also increases with velocity and vorticity magnitudes (Fig. 15).

6. Conclusion

Simulated and analyzed flow physics and effective transfer of heat in still with a single slope and studied the influence of temperature differences with appropriate plots and contour figures. There is a significant improvement in convection heat transfer of tubular stills with different water

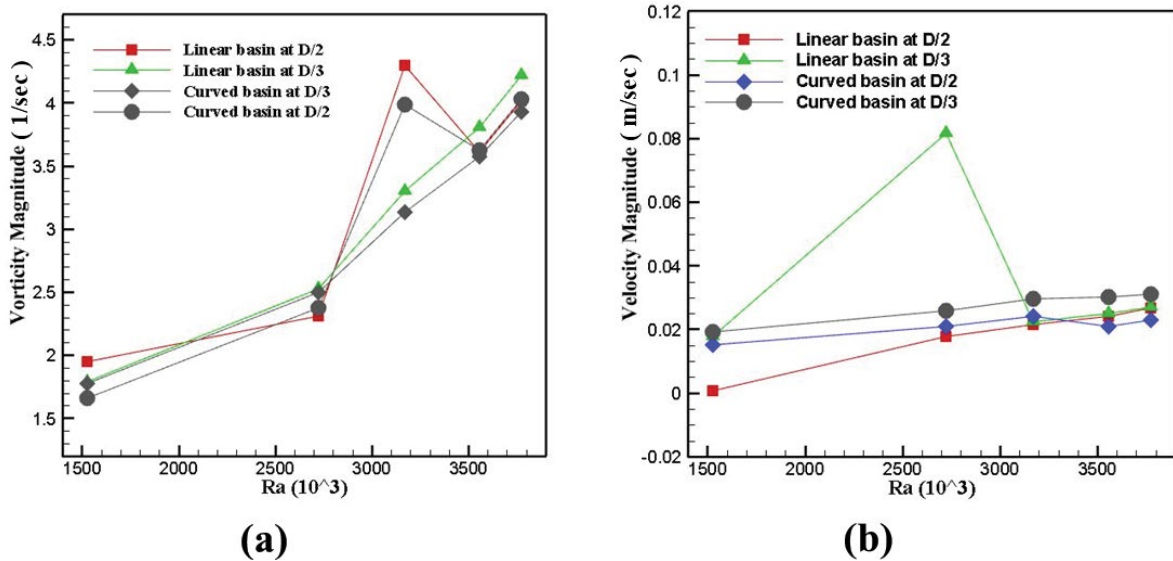


Fig. 15. Respective magnitudes of tubular solar still with different basins at variable temperature difference. (a) Vorticity magnitude (1/s) reference to Rayleigh number and (b) velocity magnitude (m/s) reference to Rayleigh number.

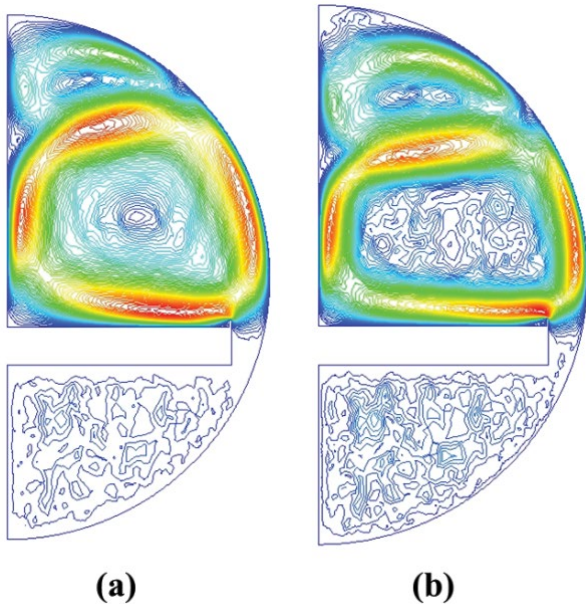


Fig. 16. Velocity contours for tubular solar still with a linear basin at $D/3$. (a) $WT = 25^\circ\text{C}$; $GT = 30^\circ\text{C}$ and (b) $WT = 55^\circ\text{C}$; $GT = 75^\circ\text{C}$.

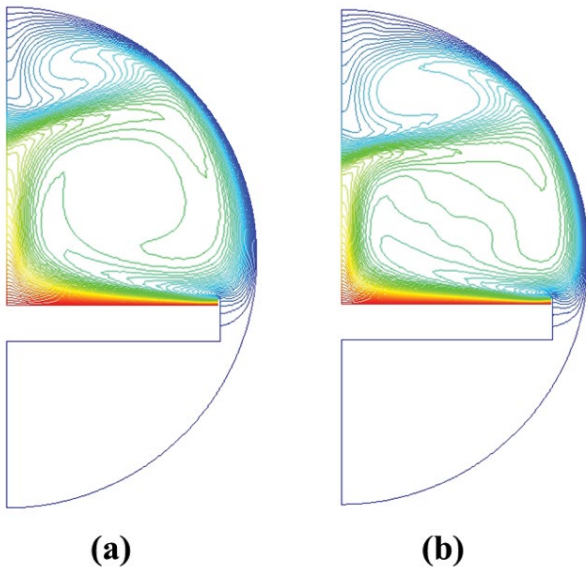


Fig. 17. Temperatures contours for tubular solar still with a linear basin at $D/3$. (a) $WT = 25^\circ\text{C}$; $GT = 30^\circ\text{C}$ and (b) $WT = 55^\circ\text{C}$; $GT = 75^\circ\text{C}$.

basins at different heights when compared with plain still. Such improvement is due to less area among the water surface and the glass curve and the advantage of flow structure with a significant increase in flow capacity. The solar still performs best when the curved water basin is at $1/2$ of the still diameter at higher Rayleigh numbers. When compared to conventional stills, the tubular still with a linear basin at $D/2$ dissipates 31.4% more heat. This means a better production rate of solar stills at higher Rayleigh numbers. The Nusselt number fluctuations are observed to be

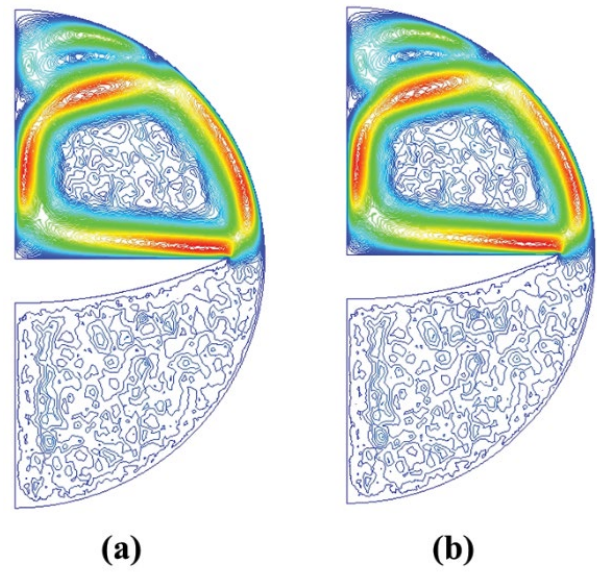


Fig. 18. Velocity contours for tubular solar still with a curved basin at $D/2$. (a) $WT = 55^\circ\text{C}$; $GT = 75^\circ\text{C}$ and (b) $WT = 65^\circ\text{C}$; $GT = 90^\circ\text{C}$.

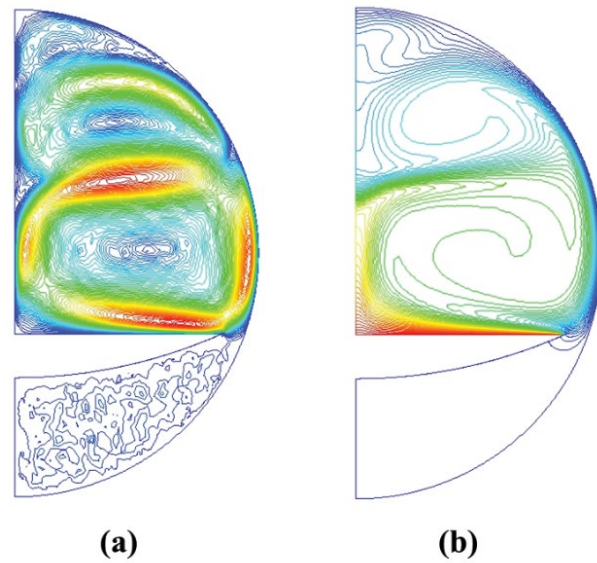


Fig. 19. Respective velocity (a) and temperature (b) contours of tubular solar still with a curved basin at $D/3$ ($WT = 55^\circ\text{C}$ and $GT = 75^\circ\text{C}$).

least when the basins are placed at $D/3$. The Nusselt number trends are almost similar for basins located at $D/2$ and $D/3$ irrespective of the basin shape. Also, the Nusselt number for either basin located at $D/3$ has fewer fluctuations and increases with Rayleigh number.

Acknowledgment

Sincere acknowledgment for the modeling and computing facilities at the Department of Mechanical Engineering,

SRMIST's Product Development Laboratory and CFD Laboratory.

Symbols

T_T	— Temperature at the top, °C
T_W	— Water surface temperature, °C
T_G	— Glass surface temperature, °C
T_B	— Temperature at bottom, °C
R_H	— Right side height, m
L_H	— Left side height, m
L_L	— Length, m
L	— Water basin length, m
H	— Water basin height, m
g	— Gravity, m/s ²
Ra	— Rayleigh number
h	— Convection heat dissipation coefficient, W/K m ²
k	— Thermal conductivity, W/K m
Nu	— Nusselt number
T	— Surface temperature, K
T_∞	— Film temperature, K
α	— Thermal diffusivity, m ² /s
ν	— Kinetic viscosity, m ² /s
β	— Thermal expansion coefficient, K ⁻¹

References

- [1] K. Sanjeev, G.N. Tiwari, Optimization of daily yield for an active double effect distillation with water flow, *Energy Convers. Manage.*, 40 (1999) 703–715.
- [2] B.I. Ismail, Design and performance of a transportable hemispherical solar still, *Renewable Energy*, 34 (2009) 145–150.
- [3] J.A. Esfahani, V. Bordbar, Double diffusive natural convection heat transfer enhancement in a square enclosure using nanofluids, *J. Nanotechnol. Eng. Med.*, 2 (2011) 021002–021009.
- [4] P.K. Abdenacer, S. Nafila, Impact of temperature difference (water-solar collector) on solar-still global efficiency, *Desalination*, 209 (2007) 298–305.
- [5] A.Z. Al-Garni, A.H. Kassem, F. Saeed, F. Ahmed, Effect of glass slope angle and water depth on productivity of double slope solar still, *J. Sci. Ind. Res.*, 70 (2011) 884–890.
- [6] V.K. Dwivedi, G.N. Tiwari, Comparison of internal heat transfer coefficients in passive solar stills by different thermal models: an experimental validation, *Desalination*, 246 (2009) 304–318.
- [7] R. Bhardwaj, M.V. ten Kortenaar, R.F. Mudde, Maximized production of water by increasing area of condensation surface for solar distillation, *Appl. Energy*, 154 (2015) 480–490.
- [8] A. Heydari, N. Rahbar, Energy and life cost analysis of a wet wall solar still with various pump working conditions, *Environ. Prog. Sustainable Energy*, 36 (2017) 532–538.
- [9] E. Papanicolaou, V. Belessiotis, Patterns of double-diffusive natural convection with opposing buoyancy forces: comparative study in asymmetric trapezoidal and equivalent rectangular enclosures, *J. Heat Transfer (ASME)*, 130 (2008) 092501–092514.
- [10] E. Papanicolaou, V. Belessiotis, Double-diffusive natural convection in an asymmetric trapezoidal enclosure: unsteady behavior in the laminar and the turbulent-flow regime, *Int. J. Heat Mass Transfer*, 48 (2005) 191–209.
- [11] S. Rashidi, M. Bovand, J.A. Esfahani, Optimization of partitioning inside a single slope solar still for performance improvement, *Desalination*, 395 (2016) 79–91.
- [12] S. Rashidi, M. Bovand, N. Rahbar, J.A. Esfahani, Steps optimization and productivity enhancement in a nanofluid cascade solar still, *Renewable Energy*, 118 (2018) 536–545.
- [13] E. Fotouhi-Bafghi, N. Rahbar, Productivity improvement of a tubular solar still, using CFD simulation, *J. Model. Eng.*, 10 (2013) 37–48 (in Persian).
- [14] N. Rahbar, J. Abolfazli Esfahani, E. Fotouhi-Bafghi, Estimation of convective heat transfer coefficient and water-productivity in a tubular solar still – CFD simulation and theoretical analysis, *Sol. Energy*, 113 (2015) 313–323.
- [15] A. Ahsan, T. Fukuhara, Mass and heat transfer model of tubular solar still, *Sol. Energy*, 84 (2010) 1147–1156.
- [16] A. Ahsan, K.M.S. Islam, T. Fukuhara, A.H. Ghazali, Experimental study on evaporation, condensation and production of a new tubular solar still, *Desalination*, 260 (2010) 172–179.
- [17] S. Subhani, R. Senthil Kumar, Numerical investigation on influence of mounting baffles in solar stills, *AIP Conf. Proc.*, 2161 (2019) 020025.
- [18] N. Rahbar, A. Asadi, E. Fotouhi-Bafghi, Performance evaluation of two solar stills of different geometries: tubular versus triangular: experimental study, numerical simulation, and second law analysis, *Desalination*, 443 (2018) 44–55.
- [19] N. Rahbar, J.A. Esfahani, Productivity estimation of a single-slope solar still: theoretical and numerical analysis, *Energy*, 49 (2013) 289–297.